# AAV-mediated transgene delivery targeting spiral ganglion nonsensory cells

Joshua S. Lin, Nhi V. Nguyen, Seiji B. Shibata

**In-situ neuronal reprogramming in the cochlea through gene therapy offers an avenue to restore hearing loss caused by neuronal damage. One possible source of neuronal conversion is the nonspiral ganglion cells (NSGCs), which include satellite cells, Schwann cells, and otic mesenchyme cells. A major obstacle for this approach is the vector-mediated transgene delivery toward NSGCs. Herein, we sought to assess the transduction profile of adeno-associated virus (AAV) serotypes with peripheral glial cell tropism in the murine inner ear. AAV-1, AAV-DJ, and AAV-PHP.eB with a cytomegalovirus promoter-driven enhanced green flourescent protein (eGFP) reporter were injected into CBA/CaJ neonatal mice via the posterior semicircular canal. One week postinjection, the cochlear tissue was collected for immunohistochemistry in whole-mount and mid-modiolar sections to assess the colocalization of eGFP within the NSGCs in the osseous spiral lamina and Rosenthal's canal. The contralateral ear served as an internal control. Auditory brain responses (ABRs) were recorded 30 days postinjection to assess for hearing loss. AAV-1 and AAV-DJ demonstrated 30–32% transduction efficacy of Pou3f4 immunopositive otic mesenchyme cells, whereas transduction efficacy of Sox2 or Sox10 positive Schwann cells and satellite cells was 0.8–1.82% for all serotypes. At 30 days postinjection, ABR thresholds in the injected mice were comparable to those of the noninjected control. We were able to transduce otic mesenchyme cells among SGNCs in the spiral ganglion region, whereas transduction of Schwann cells and satellite cells continues to pose challenges with AAV-1, AAV-DJ, and AAV-PHP.eB serotypes.** *NeuroReport* **36: 497–503 Copyright © 2025 The Author(s). Published by Wolters Kluwer Health, Inc.**

**NeuroReport** 2025, **36**:497–503

**Keywords: AAV, gene delivery, otic mesenchyme cells, Schwann cells, satellite cells**

Caruso Department of Otolaryngology – Head and Neck Surgery, University of Southern California, Los Angeles, California, USA

Correspondence to Seiji B. Shibata, MD, PhD, Caruso Department of Otolaryngology – Head and Neck Surgery, University of Southern California, 1537 Norfolk Street, Suite 5800, Los Angeles, CA 90033, USA
Tel: +1 32 3865 6148; e-mail: Seiji.Shibata@med.usc.edu

**Received** 3 March 2025 **Accepted** 16 April 2025.

## Introduction

Sensorineural hearing loss (SNHL) is the most common sensory impairment [1,2]. Although central causes can explain certain instances of SNHL, the predominant cases involve damage to mechanosensory hair cells or impairment of the auditory neurons or spiral ganglion neurons (SGNs). The SGN propagates auditory sensory signals generated by the hair cells to more upstream central nervous system targets. Primary or secondary damage to the bipolar SGN is permanent. The current paradigm to treat SNHL relies on hearing aids and cochlear implants (CIs), whose performance depends on the health and optimal number of SGN. Thus, CI outcomes are generally poor in patients with auditory neuropathy or hypoplastic auditory nerve [3,4]. Restoring hearing to individuals with significant SGN degeneration may require a regenerative therapeutic strategy.

In-situ direct reprogramming is an emerging field of regenerative research; somatic cells can bypass the pluripotent state to be converted to induced neurons (iNs), which is thought to be more efficient than reimplantation of induced pluripotent stem cells [5,6]. One potential cellular target for in-situ cellular reprogramming in the inner ear is the nonspiral ganglion cells (NSGC): including Schwann cells, satellite cells, and otic mesenchyme cells. The Schwann cells insulate the axons of the SGN in the osseous spiral lamina (OSL) and enhance action potential propagation. The satellite cells, which surround the soma of the SGNs in the Rosenthal's canal (RC) of the cochlea, perform crucial homeostatic functions to maintain the health and integrity of the SGNs. Likewise, the otic mesenchyme cells, which are the most abundant cell type in the developing inner ear, play a role in inner development, axon guidance, and SGN survival [7,8]. Importantly, NSGC survives following cochlear insults involving the sensory cells. Despite the proximity of NSGCs and SGNs, the developmental origins of the two groups differ; NSGCs originate from the neural crest, and SGNs from the otic placode. Yet, overexpression of neuronal transcription factors can coax NSGCs into SGN-like induced neurons in-vitro [5]. To realize direct reprogramming in the cochlea in-vivo neuronal transcription factors will need to be delivered selectively to the NSGC.

This is an open-access article distributed under the terms of the Creative Commons Attribution-Non Commercial-No Derivatives License 4.0 (CCBY-NC-ND), where it is permissible to download and share the work provided it is properly cited. The work cannot be changed in any way or used commercially without permission from the journal.

0959-4965 Copyright © 2025 The Author(s). Published by Wolters Kluwer Health, Inc. DOI: 10.1097/WNR.0000000000002172

AAVs have become the preferred viral vector in molecular science because of their ubiquity, ease of design [9], and relative lack of toxicity. AAVs are the current workhorse for cochlear delivery, which have been used in clinical trials for restorative inner ear gene therapy [10–13]. Prior reports showed serotype-dependent cellular tropism, permitting targeted cell delivery with chemical modification of AAV capsids. Yet, AAV tropism for tissues in the spiral ganglion area is poorly characterized [14–16]. Therefore, we investigated the following AAV capsid serotypes that have demonstrated a preference for transfection of nonsensory cells and peripheral glial cells to target NSGC [17–19]. AAV-1 transduces both sensory and supporting cells inner ear and Schwann cells [20–22]. Pseudoserotype AAV-DJ demonstrates strong supporting cell and Schwann cell tropism, while AAV-PHP.eB transfects both sensory and nonsensory cells in the cochlea, oligodendrocytes, and glial cells in the retina [23–25].

Herein, we profiled the inner ear tissue tropism of selected AAV-1, AAV-DJ, and AAV-PHP.eB serotypes focusing on the spiral ganglion region in neonatal mice. We demonstrate successful gene delivery in the otic mesenchyme cells with all vectors, with limited Schwann cell and satellite cell transduction. Our study enhances our understanding of the AAV trophic profile in NSGCs.

## Methods

### Experimental design and ethics

The experiments' animals were handled according to the American Veterinary Medical Association and the National Institue of Health standards, as the Institutional Biosafety Committee (Protocol #BUA-20–00050) and the Institutional Animal Care and Use Committee (Protocol #21248) of the University of Southern California approved each respective protocol.

### Viral vector

AAV-1, AAV-DJ, and AAV-PHP.eB serotypes were obtained from a third-party vendor (VectorBuilder Inc., Chicago, Illinois, USA); the encoded plasmid contained a cytomegalovirus (CMV) promoter encoding an enhanced green flourescent protein (eGFP) reporter gene and a woodchuck hepatitis virus posttranscriptional regulatory element. Viruses obtained had average titers of: AAV-1-eGFP at $1.83 \times 10^{12}$ gc/ml, AA-VDJ-eGFP at $1.24 \times 10^{12}$ gc/ml, and AAV-PHP.eB-eGFP at $2.91 \times 10^{12}$ gc/ml. Viral vectors were stored at −80 °C and thawed on ice before use.

### Posterior semicircular canal in neonatal mice

Wild-type inbred neonatal CBA/J mice (JAX, #000654) were selected between P3 and P5 to undergo posterior semicircular canal (PSCC) injection. The PSCC injection method is described in our previous study by Cutri *et al.* [26]. In brief, 700 nl of AAV vector suspension was mixed with 2.5% fast green dye (Sigma-Aldrich, St. Louis, Missouri, USA). The viral suspension and the dye were combined in a 10 : 1 ratio and loaded into a borosilicate glass pipette [1.5 mm outer diameter (OD) × 0.86 mm inner diameter; World Precision Instruments, Sarasota, Florida] pulled with a Sutter P-1000 micropipette puller. The final pipette had approximately 20 µml OD and was affixed to the Nanoliter 2020 injector (catalog #300704; World Precision Instruments). Hypothermic anesthesia in neonatal mice was induced with crushed ice. A postauricular incision was created and layers of muscle were dissected to expose the PSCC. The micropipette was advanced in increments using a micropipette manipulator until the PSCC was punctured to create a canalostomy, allowing the injection of vector suspension at a rate of 10 nl/s into the perilymphatic space. At the end of the injection, the incision was closed and mice were placed in a container with bedding on a heating pad for recovery before being returned to the mother. Recovery was closely monitored daily for at least three days postoperatively.

### Auditory brainstem response

Auditory brainstem responses (ABRs) were measured when the injected mice reached P30+ of age. The contralateral right ear responses served as internal controls. All animals were anesthetized with an intraperitoneal injection of ketamine (100 mg/kg) and xylazine (5 mg/kg). The ABR device was calibrated before generating auditory stimuli in each mouse. Acoustic signals were presented as tone pips with a rise and fall time of 0.5 ms and a total duration of 5 ms at frequencies 8, 16, 24, and 32 kHz. Tone pips were delivered below the threshold and then increased in 5 dB increments until an output of 90 dB sound pressure level was reached. Signals were presented at a rate of 30/s. Responses were filtered with a 0.3–3 kHz pass-band (×10 000 times). For each stimulus intensity, signals were averaged over 300 repetitions. The ABR threshold was defined as the lowest sound level at which a reproducible waveform could be observed; the peaks were measured using the ABR Peak Analysis software (Bradley Buran, Eaton-Peabody Laboratory).

### Cochlear immunohistochemistry preparations

Bilateral inner ears were harvested 1 week following PSCC injection for cochlear whole-mount sample preparation. The otic capsule was dissected from temporal bones before undergoing tissue fixation via locally perfused ice-cold 1X PBS fixed in 4% paraformaldehyde for 1 h at room temperature; the fixed capsule was then rinsed with PBS, and stored at 4 °C. Specimens were microdissected under a Leica S9i microscope before whole-mount analysis. Following permeabilization with 0.3% Triton X-100 for 10 min, the dissected cochlear whole mount segments were then immersed in a blocking solution (5% goat serum, 0.1% Triton X, 1% BSA in PBS) for 1 h at room temperature; tissues were incubated

**Fig. 1**

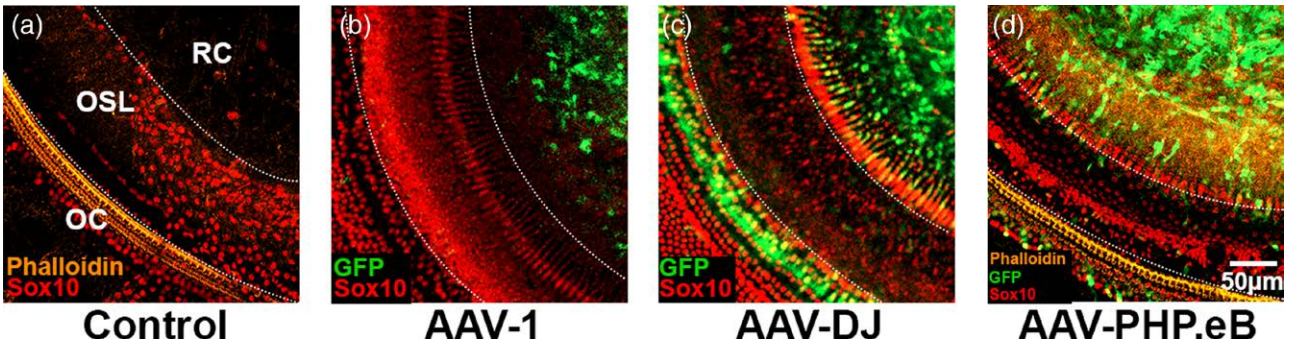


AAV-1, AAV-DJ, and AAV-PHP.eB demonstrate GFP distribution in the OSL, RC, and the OC regions in cochlear whole mount. (a–d) Control cochlear whole mount specimen with Sox10+ (red) which highlights the cochlear supporting cells in the OC and glial cells in OSL and OC area. Phalloidin+ (orange) cells delineate the cytoskeletal structure of the cochlear supporting cells and hair cells in the OC region. White dashed lines delineate the division among OC, OSL, and RC regions. (b–d) Neonatal cochleae injected with AAV-1, AAV-DJ, and AAV-PHP.eB displayed robust GFP+ signals in the OC, OSL, and RC regions at varying intensities. AAV, adeno-associated virus; OC, organ of Corti; OSL, osseous spiral lamina; RC, Rosenthal's canal.

with rabbit polyclonal anti-Sox10 antibody (1 : 200; Cell Signaling Technology, Danvers, Massachusetts, USA E6B6I #69661; Danvers, Massachusetts, USA). Subsequently, fluorescence-labeled goat anti-rabbit IgG Alexa Fluor 555 (1 : 500; Thermo Fisher Scientific, Rockford, Illinois, USA) was used as a secondary antibody for 30 min. Alexa Flour 546 Phalloidin (1 : 500; Invitrogen, Waltham, Massachusetts, USA) was used to stain F-actin for 30 min. The specimen was then embedded in 4',6-diamidino-2-phenylindole mounting media (Sigma-Aldrich).

For cryosectioning, the otic capsule was dissected from temporal bones before undergoing tissue fixation similarly as the specimen prepared for whole-mount analysis. The dissected capsules were then decalcified in 0.5 M EDTA for 24–36 h, cryoprotected in 30% sucrose for another 24–36 h, and embedded in an OCT solution. The molds were sectioned at approximately the mid-modiolar plane in 14-μm increments, which provided three measurement profiles. Serial sections were mounted on Fisherbrand super-frost charged slides and used immediately or stored at –80 °C. Following permeabilization with 0.3% Triton X-100 for 15 min, the sectioned sample was then immersed in a blocking solution (5% goat serum, 0.1% Triton X, 1% BSA in PBS) for 2 h at room temperature; tissues were incubated with rabbit polyclonal anti-Sox10 antibody (1 : 500, Cell Signaling Technology, E6B6I #69661; Danvers), rabbit polyclonal anti-Pou3f4 antibody (1 : 500; Proteus Biosciences, Ramona, California, USA), costained with mouse anti-Sox2 antibody (1 : 500; Santa Cruz Biotechnology, Dallas, Texas, USA) overnight. Subsequently, fluorescence-labeled goat anti-rabbit IgG Alexa Fluor 555 (1 : 500; Thermo Fisher Scientific) and goat anti-mouse IgG1 Alexa Fluor 647 (1 : 500; Thermo Fisher Scientific) were used as a secondary antibody for 2 h. The specimen is then embedded in mounting media (Sigma-Aldrich).

### Quantification and statistical analysis

Z-stack images of whole mounts were collected at ×10–20 on a Zeiss LSM800 confocal microscope. Maximum intensity projections of Z stacks were generated for each field of view, and images were prepared using ZEN software (Zeiss Inc.) to meet equal conditions. Each turn of the cochlea was analyzed, and the results were pooled in cell-density calculations to evaluate the colocalization of eGFP expression with the various cellular markers. The total amount of cells positive for a given cellular marker within the OSL and RC were first counted in their microscopy channel; the images were subsequently overlaid with the eGFP channel to number cells with colocalized signals. The ratios of positive eGFP signal colocalizing with each cellular marker were given as percentages to evaluate transfection efficacy. Signal colocalization was quantified with Fiji Cell Counter (NIH Image).

ABR threshold means were also averaged at each frequency described above for the left and right ears. We used two-way analysis of variance (ANOVA) analysis to compare the differences between the averages of the ABRs collected for the injected left ears and the right ears that serve as internal controls. Two-factor ANOVA and *t* tests were conducted using Microsoft Excel. Statistical significance was defined at $P$ less than 0.05.

## Results

### AAV-1, AAV-DJ, and AAV-PHP.eB transduce cells in the Rosenthal's canal area and osseous spiral lamina in whole mount tissue

Cochlear histology was evaluated with whole-mount preparation 7 days postinjection (dpi). We qualitatively

assessed eGFP expression in the various cochlear structures, with the contralateral ears serving as internal controls. In whole-mount preparation, we observed robust eGFP expression in cochlear areas corresponding with OSL and RC in cochlear tissues transfected with AAV-1, AAV-DJ, and AAV-PHP.eB (Figs. 1b–d). AAV-PHP.eB demonstrated greater cellular transduction in the OSL and SGN cells in the RC area. AAV-1 transduction is localized to the RC area, while AAV-DJ transduces the inner pharyngeal cells in the organ of the Corti (OC) and the RC area. All the vectors demonstrated varying degrees of colocalization with Sox10+ cells in the whole-mount preparation; however, the complex spatial arrangement of the cochlear tissue in the OSL and RC area complicates quantifying cellular GFP and Sox10 colocalization in whole-mount tissue. We further analyzed the tissues that had undergone cryosection preparation. No eGFP signal was observed in the contralateral control ears.

### Pou3f4+ mesenchymal cells are preferentially transfected by AAV-1, AAV-DJ, and AAV-PHP.eB, whereas Sox2+/10+ Schwann cell and satellite cell transfection is limited

We analyzed mid-modiolar cochlear tissue of the cryosection sample 7dpi. Aside from the cochlear glia, the abundant otic mesenchymal cells potentially serve as another primary cell source of in-vivo direct neuronal reprogramming [5]. While the precise function of otic mesenchyme remains contentious and unknown, these cells readily express Pou3f4. AAV-1 and AAV-DJ demonstrated extensive eGFP expression in the Pou3f4+ otic mesenchymal cells in RC and OSL areas. The transfection rate was 30.1% for AAV-1 and 32.5% for AAV-DJ; we did not determine a significant difference between the two ($P = 0.66$). Conversely, AAV-PHP.eB had a modest tropism towards the Pou3f4+ cells (10.1%); the difference in Pou3f4+ cell transfection is significantly less for AAV-PHP.eB than those seen with AAV-1 and AAV-DJ (Fig. 2a and d, $P < 0.001$, $P < 0.05$, respectively).

The AAV-1 mediated eGFP signals had limited colocalization rates of 1.83% with Sox10+ and 0.90% with Sox2+ cells. AAV-DJ showed similar distribution levels of eGFP expression in the RC, OSL, area with colocalization of eGFP and Sox10+ or Sox2+ cells at 1.2 and 0.88% (Fig. 2b–d). Analyzing a small quantity of colocalized cells, AAV-DJ has a tendency to transfect both Sox10+ Schwann cells in the OSL and satellite cells in the RC. While AAV-1 tends to transfect satellite cells in the RC and not Schwann cells in the OSL. In AAV-PHP.eB injected cochlea, the amount of Sox10 (1.82%) and Sox2 (1.39%) transduction was comparable to AAV-1 and DJ. Of note, AAV-PHP.eB predominantly transduced to SGN in the RC (Fig. 2b and c).

### Adeno-associated virus vectors do not alter hearing thresholds after neonatal posterior semicircular canal injections

We analyzed ABR thresholds following PSCC injections in neonatal mice at 30 dpi. ABR thresholds of all mice were measured at 8, 16, 24, and 32 kHz, with the contralateral right ear serving as an internal control. We did not observe significant ABR threshold differences among AAV-injected and uninjected ears (Fig. 3, $n = 11$, $P \geq 0.09$). These results imply that the potential effect of injecting the AAV vectors on the auditory physiology of wild-type CBA/CaJ mice is negligible. We did not observe postsurgical complications or weight loss in the injected neonatal mice. We identify PSCC injections in neonatal mice as a safe and effective injection method.

## Discussion

This study aimed to characterize the transduction profile of AAV-1, AAV-DJ, and AAV-PHP.eB serotypes in the spiral ganglion region of the neonatal CBA/CaJ wild-type mice. We demonstrated that a single PSCC injection of the viral suspension leads to robust transgene expression in the neonatal mouse cochlea. We demonstrate that AAV-1 and AAV-DJ serotypes preferentially transfect the Pou3f4+ otic mesenchymal cells; however, the overall transduction efficacy of Sox2+/10+ Schwann cells and satellite cells remained low with all serotypes, contrary to our qualitative analysis of the NGSCs with the whole-mounts. Care should be taken when assessing cellular tropism in the spiral ganglion region with whole mounts alone. Lastly, we demonstrate that PSCC injection during the neonatal period is well tolerated and does not impair hearing which is consistent with prior reports [18].

AAVs are widely used for inner ear transgene delivery. Most efforts have focused on establishing the transduction profiles of various recombinant AAV serotypes targeting the mechanosensory hair cells and supporting cells in the OC. Still, there is comparatively less emphasis on targeting the NSGCs. To our knowledge, we are the first to describe that the Pou3f4+ otic mesenchyme cells are transfected with AAV-DJ and AAV-1. Recent studies have illustrated that Pou3f4+ otic mesenchyme cells are crucial in inner ear development and contribute to the regulation of spiral ganglion axon fasciculation [27] and are essential in promoting SGN survival in the postnatal mouse cochlea [7]. The *POU3f4* gene is a Pit-Oct-Unc-domain transcription factor, widely expressed in otic mesenchymal cells and associated with human X-linked hearing loss (DFNX2), which results in inner and middle ear malformation in mice and humans [28]. Furthermore, Noda *et al.* [5] demonstrated the feasibility of neural reprogramming of otic mesenchymal cells into induced neurons with a combination of proneuronal transcription factor Ascl1 and NeuroD1 in-vitro, demonstrating that otic mesenchymal cells are a viable source for direct neural reprogramming.

**Fig. 2**

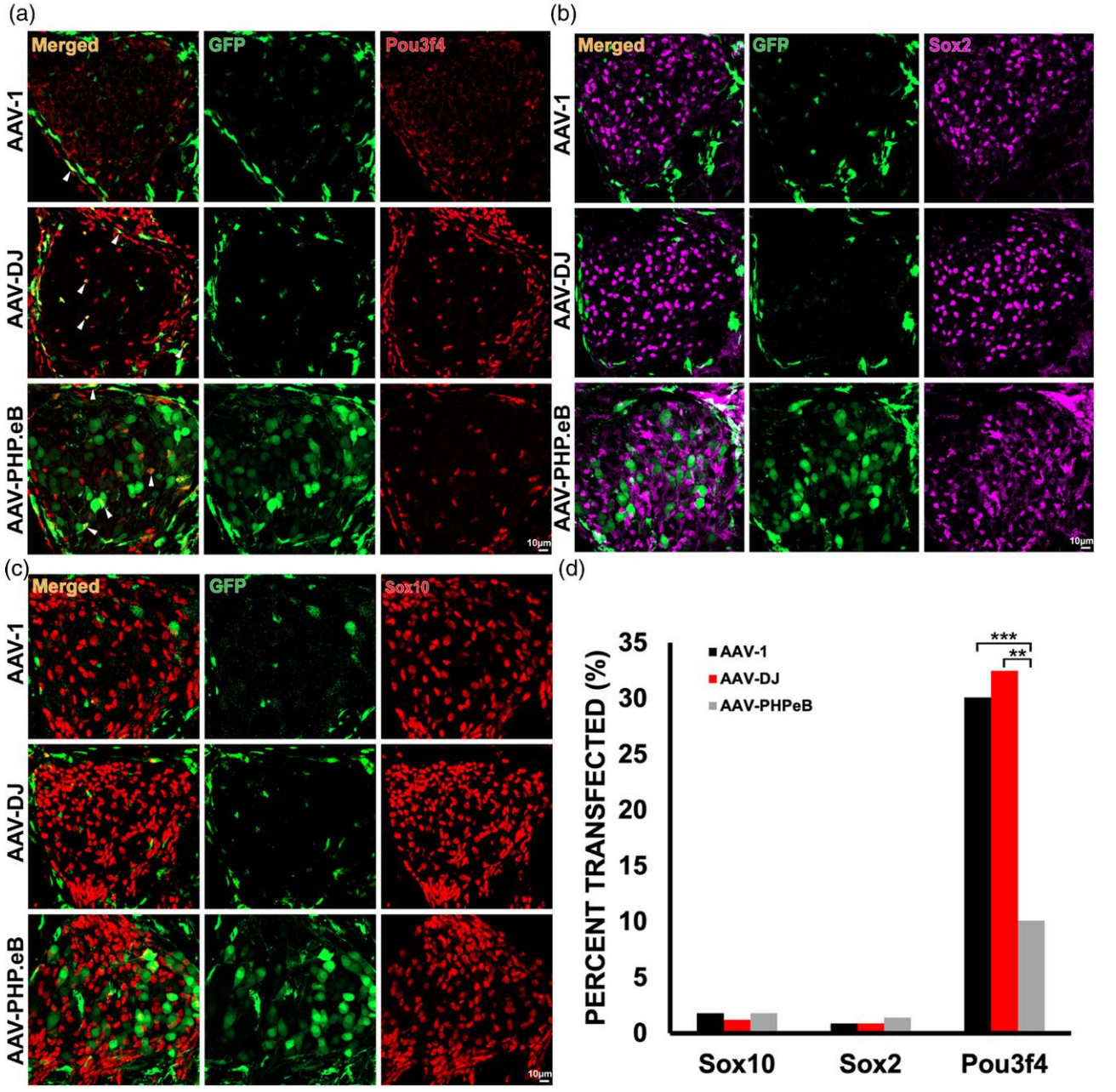


Pou3f4+ mesenchymal cells are preferentially transfected by AAV-1 and AAV-DJ. (a) AAV serotypes mediated GFP expression colocalized with Pou3f4+ (red) cells. (b) AAV serotypes also demonstrated transfected-GFP expression that colocalized with a few Sox2+ (magenta) cells. (c) AAV-DJ and AAV-PHP.eB demonstrated AAV-mediated GFP expression colocalizing with a few Sox10+ (red) cells. The non-Sox2/10 positive cells in the RC represent SGN cells. (d) Transfection efficacy of the selected AAV vectors regarding Sox10+, Sox2+, and Pou3f4+ cells. AAV-1, AAV-DJ and AAV-PHP.eB transfects 1.20–1.82% of the Sox10+ cells within the RC. White arrowheads depict areas with colocalized GFP and Sox2/10 or Pou3f4 signals. The Sox2+ cells were 0.88–1.39%, respectively. AAV-1 and AAV-DJ transfection ratio of Pou3f4 was 30.1 and 32.5%, whereas AAV-PHP.eB was 10.1%. ** Denotes significant level *P* less than 0.0 and *** denotes significance level *P* less than 0.001. AAV, adeno-associated virus; RC, Rosenthal's canal; SGN, spiral ganglion neuron.

We demonstrate that cochlear injection of AAV-DJ and AAV-1 with a ubiquitous CMV promoter led to a 30–32% transfection efficacy of the otic mesenchyme, compared with the 10.1% by AAV-PHP.eB. Higher transduction efficiency with our vectors may be desirable to maximize the therapeutic potential of neural reprogramming in the inner ear. Yet, increased AAV transduction may not be necessary, as the transfection rate of 10–15% was

**Fig. 3**

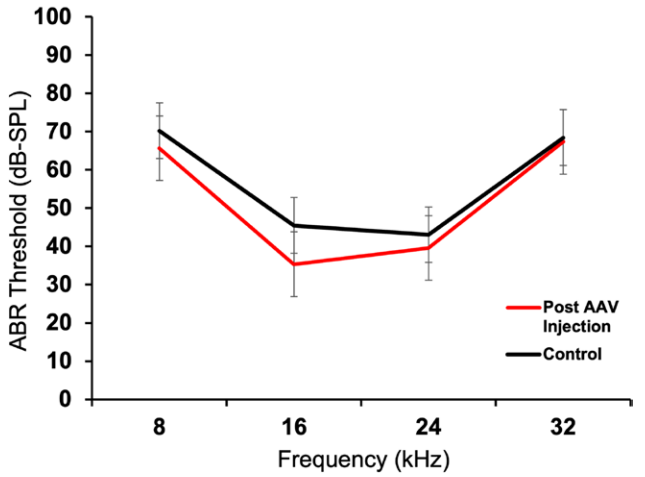


Threshold shifts are not significantly elevated in mice injected with AAV-1, AAV-DJ, and AAV-PHP.eB via posterior semicircular canal. The left ears of mice injected with AAV-1, AAV-DJ, and AAV-PHP.eB were averaged and compared to those of uninjected contralateral ears ($n = 11$) at 30 dpi. Injected ears (red) have thresholds comparable to those of uninjected control mice (black), with no statistical difference ($P = 0.09$). This indicates that PSCC is well-tolerated in neonatal mice. AAV, adeno-associated virus; dpi, days postinjection; PSCC, posterior semicircular canal.

adequate for restoring hearing in deaf Whirler mice using AAV gene therapy, and in some cases, enhanced expression of the transgene can also lead to cochlear toxicity [10,29]. Therefore, we conclude that AAV-DJ and AAV-1 are promising candidates to target otic mesenchyme cells for direct neuronal reprogramming. Alternatively, AAV-DJ and AAV-1 may also be utilized to deliver neurotrophic factors to otic mesenchyme cells for enhanced cochlear health and protection from noise-induced hearing loss, or rescue of phenotypes associated with *POU3f4* deficiencies in DFNX2.

Our study reveals that Sox2/10 cells in the OSL and RC areas were minimally transfected with AAV-1, AAV-DJ, and AAV-PHP.eB ranging from 0.88 to 1.82% at 7 dpi. With regards to the relatively low transfection efficacy of the selected viral capsids, the eGFP reporter gene delivered by AAV-1, AAV-DJ, and AAV-PHPeB did not exceed more than 5% of the colocalization with glial cells, suggesting that tropic preference towards the peripheral glial cells in the inner ear is limited. Previous reports have shown that AAV-1, AAV-DJ, and PHP.eB can transfect the supporting cells of the organ of Corti and Schwann cells and satellite cells in other systems [28]. These findings led us to hypothesize that these vectors would have tropism toward NSGCs because supporting cells share the same glial markers as Schwann cells and satellite cells, such as Sox2, Sox10, and Plp, and are transcriptionally similar [29]; however, despite these phenotypic similarities, the regional environment in the cochlea differs. The supporting cell surfaces are readily accessible to the AAV vectors through the cochlear fluids, while Schwann cells and satellite cells are encased in the bony, but porous, modiolus. We speculate that this physical barrier hinders the penetration and access of the AAVs to the surface receptors of Schwann cells and satellite cells, leading to a low transfection rate of Schwann cells and satellite cells. This may also explain why the otic mesenchyme cells, situated closer to the surface of the scala tympani, are more preferentially transfected. Lastly, we did observe AAV-PHP.eB transfection of the SGNs adjacent to Schwann cells and satellite cells, suggesting that viral capsid design and modification may contribute to overcoming physical barriers in the cochlea.

To conclude, we demonstrate that AAV-1 and AAV-DJ serotypes are promising vectors to transfect the Pou3f4+ otic mesenchymal cells. Future efforts should include screening for other AAV serotypes, designing tissue-specific viral capsids, and using more selective promoters to increase the selectivity and efficacy of targeting NSGCs.

## Acknowledgements

We want to acknowledge the Optical Imaging Facility of Broad Stem Cell Research Center for assistance in image acquisition. J.S.L. was supported by the National Institute of Health-Clinician Scientist Training Program (R25DC019700). S.B.S. was supported by funding from the National Institute for Deafness and Communication Disorders (NIDCD) K08DC021750, the AOS Clinician-Scientist Award, and the TRIO Career Development Grant.

### Conflicts of interest

There are no conflicts of interest.

## References

1 Huang AR, Jiang K, Lin FR, Deal JA, Reed NS. Hearing loss and dementia prevalence in older adults in the US. *JAMA* 2023; **329**:171–173.
2 Choi JS, Adams ME, Crimmins EM, Lin FR, Ailshire JA. Association between hearing aid use and mortality in adults with hearing loss in the USA: a mortality follow-up study of a cross-sectional cohort. *Lancet Healthy Longev* 2024; **5**:e66–e75.
3 Shearer AE, Hansen MR. Auditory synaptopathy, auditory neuropathy, and cochlear implantation. *Vol. 4. Laryngoscope investigative otolaryngology*. John Wiley and Sons Inc.; 2019. pp. 429–440.
4 Lin PH, Wu HP, Wu CM, Chiang YT, Hsu JS, Tsai CY, *et al.* Cochlear implantation outcomes in patients with auditory neuropathy spectrum disorder of genetic and non-genetic etiologies: a multicenter study. *Biomedicines* 2022; **10**:1523.
5 Noda T, Meas SJ, Nogami J, Amemiya Y, Uchi R, Ohkawa Y, *et al.* Direct reprogramming of spiral ganglion non-neuronal cells into neurons: toward ameliorating sensorineural hearing loss by gene therapy. *Front Cell Dev Biol* 2018; **6**:16.
6 Nishimura K, Weichert RM, Liu W, Davis RL, Dabdoub A. Generation of induced neurons by direct reprogramming in the mammalian cochlea. *Neuroscience* 2014; **275**:125–135.
7 Brooks PM, Rose KP, MacRae ML, Rangoussis KM, Gurjar M, Hertzano R, Coate TM. Pou3f4-expressing otic mesenchyme cells promote spiral ganglion neuron survival in the postnatal mouse cochlea. *J Comp Neurol* 2020; **528**:1967–1985.

8 Rose KP, Manilla G, Milon B, Zalzman O, Song Y, Coate TM, Hertzano R. Spatially distinct otic mesenchyme cells show molecular and functional heterogeneity patterns before hearing onset. *iScience* 2023; **26**:107769.

9 Han J, Zhu L, Zhang J, Guo L, Sun X, Huang C, *et al*. Rational engineering of adeno-associated virus capsid enhances human hepatocyte tropism and reduces immunogenicity. *Cell Prolif* 2022; **55**:e13339.

10 Iwasa Y, Klimara MJ, Yoshimura H, Walls WD, Omichi R, West CA, *et al*. Mutation-agnostic RNA interference with engineered replacement rescues Tmc1-related hearing loss. *Life Sci Alliance* 2023; **6**:e202201592.

11 Takada Y, Beyer LA, Swiderski DL, O'Neal AL, Prieskorn DM, Shivatzki S, *et al*. Connexin 26 null mice exhibit spiral ganglion degeneration that can be blocked by BDNF gene therapy. *Hear Res* 2014; **309**:124–135.

12 Tarabichi O, Correa T, Kul E, Phillips S, Darkazanly B, Young SM, Hansen MR. Development and evaluation of helper dependent adenoviral vectors for inner ear gene delivery. *Hear Res* 2023; **435**:108819.

13 Wang Y, Qiao L, Chen Y, Wen L, Yue B, Qiu J, Wu S. Establishment of a model of cochlear lesions in rats to study potential gene therapy for sensorineural hearing loss. *Int J Pediatr Otorhinolaryngol* 2015; **79**:2147–2154.

14 Xue Y, Tao Y, Wang X, Wang X, Shu Y, Liu Y, *et al*. RNA base editing therapy cures hearing loss induced by OTOF gene mutation. *Mol Ther* 2023; **31**:3520–3530.

15 Yoshimura H, Shibata SB, Ranum PT, Moteki H, Smith RJH. Targeted allele suppression prevents progressive hearing loss in the mature murine model of human TMC1 deafness. *Mol Ther* 2019; **27**:681–690.

16 Omichi R, Yoshimura H, Shibata SB, Vandenberghe LH, Smith RJH. Hair cell transduction efficiency of single- and DUAL-AAV serotypes in adult murine cochleae. *Mol Ther Methods Clin Dev* 2020; **17**:1167–1177.

17 Yamazaki Y, Hirai Y, Miyake K, Shimada T. Targeted gene transfer into ependymal cells through intraventricular injection of AAV1 vector and long-term enzyme replacement via the CSF. *Sci Rep* 2014; **4**:5506.

18 György B, Sage C, Indzhykulian AA, Scheffer DI, Brisson AR, Tan S, *et al*. Rescue of hearing by gene delivery to inner-ear hair cells using exosome-associated AAV. *Mol Ther* 2017; **25**:379–391.

19 Barbosa Spinola CM, Boutet de Monvel J, Safieddine S, Lahlou G, Etournay R. In utero adeno-associated virus (AAV)-mediated gene delivery targeting sensory and supporting cells in the embryonic mouse inner ear. *PLoS One* 2024; **19**:e0305742.

20 Hoyng SA, De Winter F, Gnavi S, van Egmond L, Attwell CL, Tannemaat MR, *et al*. Gene delivery to rat and human Schwann cells and nerve segments: a comparison of AAV 1-9 and lentiviral vectors. *Gene Ther* 2015; **22**:767–780.

21 Shu Y, Tao Y, Wang Z, Tang Y, Li H, Dai P, *et al*. Identification of adeno-associated viral vectors that target neonatal and adult mammalian inner ear cell subtypes. *Hum Gene Ther* 2016; **27**:687–699.

22 Liu Y, Okada T, Sheykholeslami K, Shimazaki K, Nomoto T, Muramatsu SI, *et al*. Specific and efficient transduction of cochlear inner hair cells with recombinant adeno-associated virus type 3 vector. *Mol Ther* 2005; **12**:725–733.

23 Fukui Y, Morihara R, Hu X, Nakano Y, Yunoki T, Takemoto M, *et al*. Suppression of PTBP1 in hippocampal astrocytes promotes neurogenesis and ameliorates recognition memory in mice with cerebral ischemia. *Sci Rep* 2024; **14**:20521.

24 Yuan M, Tang Y, Huang T, Ke L, Huang E. In situ direct reprogramming of astrocytes to neurons via polypyrimidine tract-binding protein 1 knockdown in a mouse model of ischemic stroke. *Neural Regen Res* 2024; **19**:2240–2248.

25 O'Carroll SJ, Cook WH, Young D. AAV targeting of glial cell types in the central and peripheral nervous system and relevance to human gene therapy. *Front Mol Neurosci* 2020; **13**:618020.

26 Cutri RM, Lin J, Nguyen NV, Shakya D, Shibata SB. Neomycin-induced deafness in neonatal mice. *J Neurosci Methods* 2023; **391**:109852.

27 Coate TM, Raft S, Zhao X, Ryan AK, Crenshaw EB, Kelley MW. Otic mesenchyme cells regulate spiral ganglion axon fasciculation through a Pou3f4/EphA4 signaling pathway. *Neuron* 2012; **73**:49–63.

28 Samadi DS, Saunders JC, Crenshaw EB. Mutation of the POU-domain gene Brn4/Pou3f4 affects middle-ear sound conduction in the mouse. *Hear Res* 2005; **199**:11–21.

29 Chien WW, Isgrig K, Roy S, Belyantseva IA, Drummond MC, May LA, *et al*. Gene therapy restores hair cell stereocilia morphology in inner ears of deaf whirler mice. *Mol Ther* 2016; **24**:17–25.